

# Burning Properties of Aluminum in H<sub>2</sub>O and CO<sub>2</sub>

Julian J. Lee and Fan Zhang

Defence Research and Development Canada - Suffield, AB, Canada

Corresponding author, J.J. Lee: [julian.lee@drdc-rddc.gc.ca](mailto:julian.lee@drdc-rddc.gc.ca)

## 1. Introduction

Renewed interest in non-ideal explosives has prompted the present investigation of ignition and burning mechanisms of aluminum particles in hot combustion products. By injecting the particles directly into gaseous hot combustion products, the ignition delay and burn time are measured for a wide range of pressures, temperatures, and particle sizes. The oxidizing effect of H<sub>2</sub>O vapor and CO<sub>2</sub> are investigated individually by burning mixtures of H<sub>2</sub>/O<sub>2</sub>/N<sub>2</sub>, and CO/O<sub>2</sub>/N<sub>2</sub> respectively. Using a piston-driven injection technique, the particles are introduced at a velocity of less than 15 m/s into quiescent combustion products following complete burning of a gaseous mixture by flame in a closed spherical vessel. Using the present method, the combustion properties of the particles can be studied at relatively constant pressure and temperature. By varying the initial pressure of the gaseous mixture and the fraction of nitrogen dilution, a wide range of product pressures and temperatures are investigated.

## 2. Background and Issues

The combustion properties of aluminum particles have been the subject of many studies (Friedman & Macek 1962, Gurevich et al. 1970, 1978, Razdobreev et al. 1976, Derevyaga et al. 1977, Boiko et al. 1987, Rozenband & Vaganova 1992). The combustion properties of 22- $\mu$ m and 53- $\mu$ m aluminum particles have been studied in the context of solid rocket propellant applications for products of H<sub>2</sub>/O<sub>2</sub>/N<sub>2</sub> using a method similar to that used in the present study (Foelsche et al. 1998). The oxidizing efficiency of specific gaseous products consisting of H<sub>2</sub>O and CO<sub>2</sub> has also been studied for 5-10  $\mu$ m aluminum particles in a shock tube apparatus (Servaites et al. 2001).

Non-ideal explosions can occur in partially-confined environments where shock reflection and diffraction can influence the particle combustion. Due to shock heating and expansion cooling of the detonation products, the conditions of particle burning differ from the high pressures and temperatures typically encountered in solid rocket propellant burning. In this work, we investigate the mechanisms of aluminum particle burning in ranges of pressure, temperature, and flow conditions that differ from typical propellant burning conditions.

We seek to understand the ignition and energy release mechanisms of aluminum particles in various oxidizers under these burning conditions. To establish the foundations necessary to reach this objective, we systematically investigate the burning properties of atomized aluminum particles at quiescent conditions from 2-30  $\mu$ m in H<sub>2</sub>O and CO<sub>2</sub> at pressures from 6-80 atm and temperatures from 1500-2700 K. Specific issues of interest are the oxidizing efficiency of H<sub>2</sub>O relative to CO<sub>2</sub>, the difference between results obtained in a shock tube and from particle injection into a quiescent gas, scaling effect of particle size.

### 3. Experimental Details

#### 3.1 Experimental Setup

The experimental apparatus consists of a 23-liter combustion vessel with an internal spherical shape (Figure 1). The vessel was designed to withstand static pressures up to 1000 atm. After the chamber is evacuated then filled with a premixed combustible gas mixture, a flame is ignited with an exploding wire across the gap of a spark igniter. When the gaseous mixture is completely burned, a small amount of aluminum particles (~2 mg) are injected into the gaseous combustion products with a particle injector based on the design of Foelsche et al. (1999). This design allows the particles to be injected into the chamber after the gaseous mixture has been completely burned. An electrical switch is connected to the injector to indicate the moment that the particles have been injected. The pressure within the chamber is monitored with a Kulite HKS-375 transducer, and the combustion light is monitored with a broadband silicon photo-detector through a fiber-optic cable inserted into the chamber.

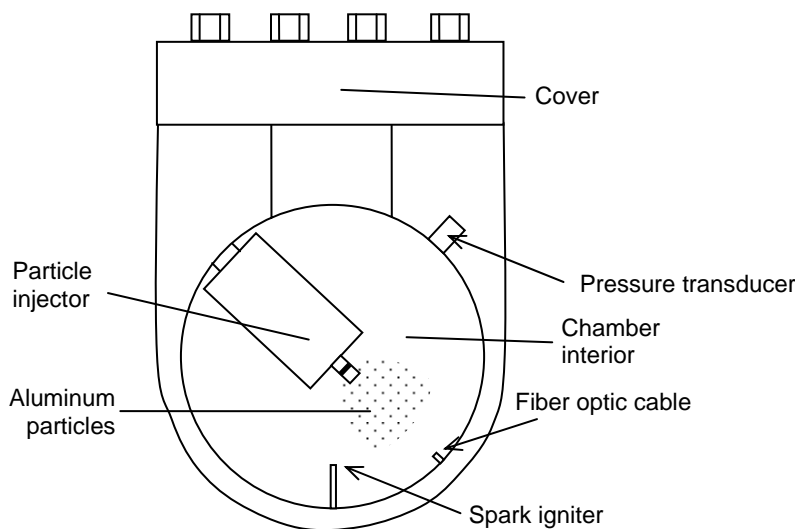


**Figure 1. Schematic diagram of combustion vessel.**

To generate combustion products consisting mostly of H<sub>2</sub>O vapor, a mixture of H<sub>2</sub> and air with an equivalence ratio ( $\phi$ ) of 0.9 was used. For products consisting mostly of CO<sub>2</sub>, a mixture of CO and air with  $\phi = 0.9$  was used. The equivalence ratio of 0.9 was chosen by performing thermo-chemical equilibrium calculations with the CEA code (Gordon 1996) and choosing a mixture for which the combustion products contained the smallest amounts of all species except for the desired product of H<sub>2</sub>O or CO<sub>2</sub>. The final pressure of the combustion products was varied by changing the initial pressure of the combustible mixture. The temperature of the products was lowered by adding N<sub>2</sub> dilution.

The particles used were H-series spherical aluminum powders supplied by Valimet. The physical characteristics of the powders as given by the manufacturer are shown in Table 1 below.

The maximum and minimum sizes were measured by the manufacturer using aerodynamic particle sizing.

**Table 1. Table of sizes for Valimet spherical aluminum powders**

Type	Nominal Size ( $\mu\text{m}$ )	Minimum Size ( $\mu\text{m}$ )	Maximum Size ( $\mu\text{m}$ )
H-5	5	4.5	7.0
H-10	10	8.0	12.0
H-15	15	14.0	18.0
H-30	30	20.0	30.0

### 3.2 Measurement of Ignition Delay

A typical test began with the ignition of the gas mixture, causing a gradual increase in the pressure within the chamber as the flame propagated through the gas (Figure 2). When the burning reached completion, the pressure reached a maximum, then gradually decayed as the combustion products cooled. Slightly before maximum pressure was reached, a diaphragm in the particle injector burst and allowed high pressure products to enter the injector and drive a piston containing the particles. The piston reached a maximum speed as it extended into the combustion products, releasing and dispersing the particles a few milliseconds after complete burning of the gases. The maximum pressure was typically about 75-90% of the constant volume combustion pressure calculated with the thermo-chemical equilibrium code CEA (Gordon 1996). For mixtures with a lower flame speed, the pressure deficit was larger due to larger heat losses to the chamber walls.

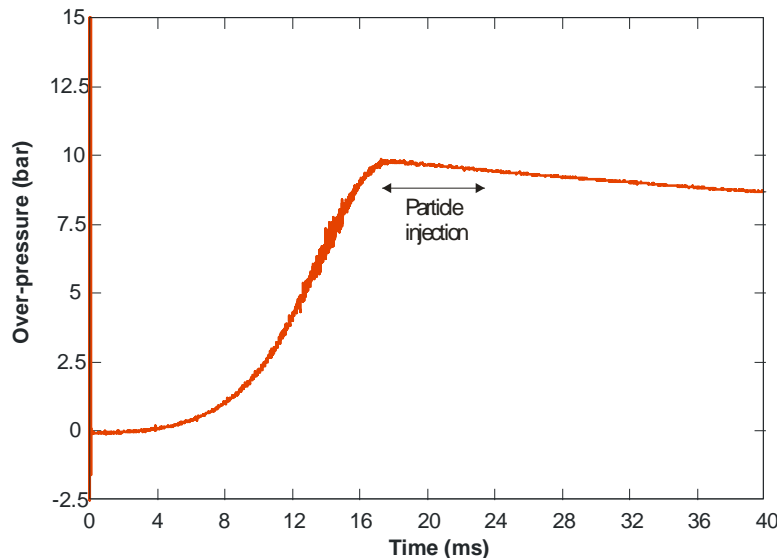


**Figure 2. Typical pressure history for burning of an  $\text{H}_2$ -air mixture with  $\phi = 0.9$  and an initial pressure of 1.66 bar. Particles are injected shortly after completion of burning at maximum pressure.**

When the piston was fully extended, the particles were exposed to the gaseous combustion products. An electric switch was triggered by the piston at this instant (Figure 3), indicating the moment of particle injection. After injection, the dispersed aluminum particles ignited after a

certain delay, causing a detectable increase in light intensity in the chamber. Hence the illumination from the burning aluminum caused a strong peak in light intensity above the background light from the hot gases. The ignition delay was taken as the time between the moment of particle injection to the beginning of the increase in light due to aluminum burning. A photo-detector trace from a background test where no particles were loaded into the injector is shown for comparison. In this trace, the signal increased slightly due to the radiation from the hot gaseous products, but no second peak was visible, showing that aluminum burning generates a distinct peak in the photo-detector signal.

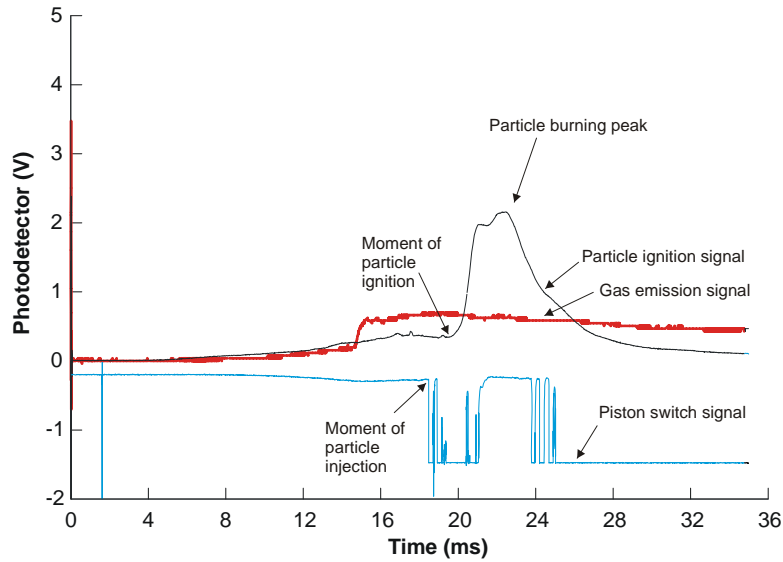


**Figure 3. Photo-detector signal showing light intensity from combustion of particles (particle ignition signal). The gas emission signal shows the light emission from gas combustion without particles present. The piston switch signal indicates the moment particles are injected into the gas by the piston.**

#### 4. Preliminary Results and Discussion

Based on experimental results obtained to date, a number of observations can be made on the induction time of aluminum particles in  $H_2O$  or  $CO_2$ . The first is that the induction time at a pressure of about 10.8 bar increased from approximately 3 ms to 9 ms as the particle size increased from about  $5 \mu m$  to  $30 \mu m$  (Figure 4). This figure shows the induction time as a function of the nominal particle size in water vapor or  $CO_2$ . These induction times are comparable to those measured by Foelsche et al. (1998) who studied aluminum burning at higher pressures above 38 bar, but are significantly longer by a factor of about five for similar particle sizes. This difference cannot be accounted for by the pressure dependence of induction time ( $t_{ign}$ ) proposed by Foelsche et al. (1998):

$$t_{ign} = 6.8 p_c^{-0.6}$$

where  $p_c$  is the pressure in atmospheres and  $t_{ign}$  is given milliseconds. Another factor supporting longer induction times in the present experiments is the much smaller mole fractions of species besides the main product. In the present experiment, the percentage of mole fractions of other

potentially oxidizing species such as  $O_2$ ,  $OH$ , and  $NO$  were below 2% as compared with about 20%  $O_2$  in Foelsche's experiment. Another observation is that the induction times in  $H_2O$  and  $CO_2$  are nearly identical (Figure 4). This does not agree with past studies using a shock tube (Servaites et al. 2001) where the induction time in  $H_2O$  has been found to be 3-6 times longer than in  $CO_2$ . This suggests that the ignition process in the present experiment where the particles are injected at a relatively low speed into a quiescent gas differs significantly from ignition in a shock tube. In the absence of shock waves in the present experiment, the  $Al_2O_3$  coating on the particles may remain intact and inhibit ignition and burning. Another supporting factor for the longer induction times is that convective heat transfer rate is much lower in the present experiment due to the low speed of the particles as compared to the shock tube experiment. The particle heating would therefore be longer, again leading to longer induction times. These factors remain to be verified.

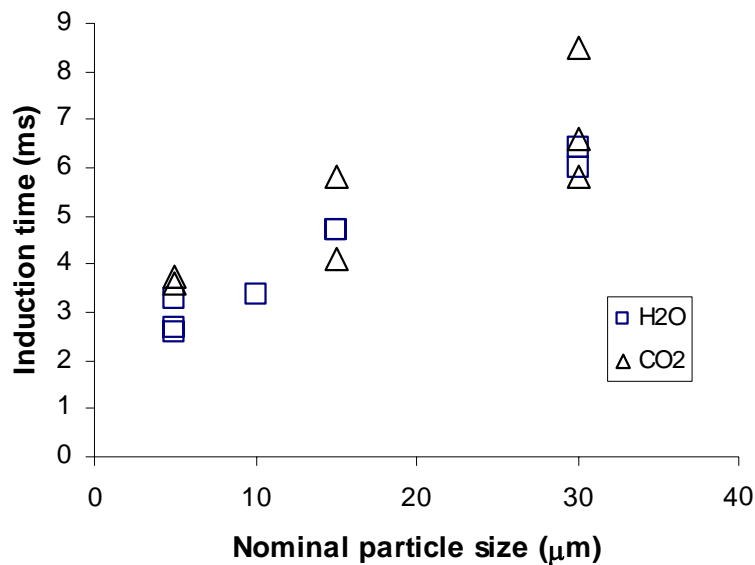


**Figure 4. Induction time for aluminum particle burning in combustion products of  $H_2O$  or  $CO_2$  at 10.8 bar.**

To date, two combustion pressures have been investigated: 6.5 and 10.8 bar (Figure 5). As previously observed and expected, the induction time increased from approximately 3 ms to 9 ms as the particle size increased from about 5  $\mu m$  to 30  $\mu m$ . It was found that at these two pressures, the induction time was the same. This suggests that the induction time is not a strong function of pressure within this range.

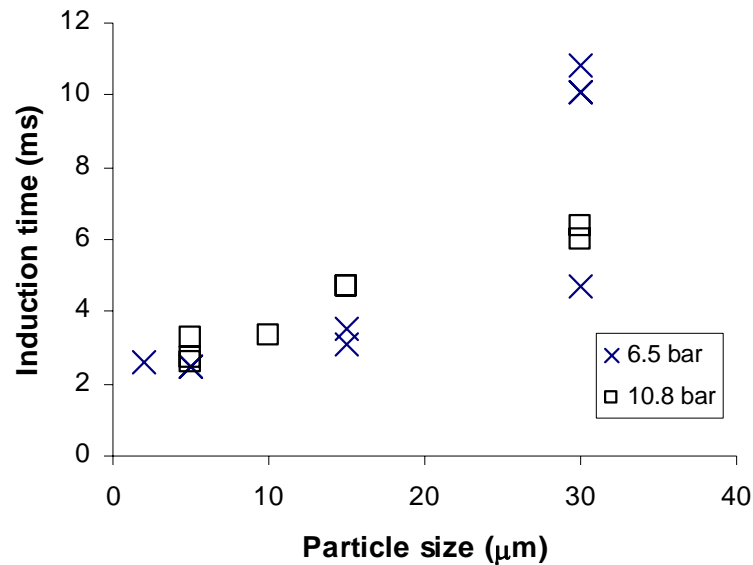


Figure 5. Induction time dependence on particle size in H<sub>2</sub>O at 6.5 and 10.8 bar.

### Acknowledgements

The authors would like to thank S. Wong, K. Gerrard, D. Boechler, and A. Nickel for their valuable technical assistance in performing the experiments.

### References

- R. Friedman and A. Macek 1962 *Ignition and combustion of aluminum particles in hot ambient gases*, Combust. Flame 6:9-19.
- M.A. Gurevich, K.I. Lapkina and E.S. Ozerov 1970 *Ignition limit of aluminum particles*, Combustion, Explosion, and Shock Waves, Vol. 6, No. 2, 172-175.
- A.A. Razdobreev, A.I. Skorik and Yu.V. Frolov 1976 *Ignition and combustion mechanism in aluminum particles*, Combustion, Explosion, and Shock Waves, Vol. 12, No. 2, 203-208.
- M.E. Derevyaga, L.N. Stesik and E.A. Fedorin 1977 *Ignition and combustion of aluminum and zinc in air*, Combustion, Explosion, and Shock Waves, Vol. 13, No. 6, 852-857.
- M.A. Gurevich, E.S. Ozerov and A.A. Yurinov 1978 *Effect of an oxide film on the inflammation characteristics of aluminum*, Combustion, Explosion, and Shock Waves, Vol. 14, No.4, 50-55.
- V.M. Boiko, A.V. Fedorov, V.M. Formin, A.N. Papyrin and R.I. Soloukhin 1987 *Ignition of small particle behind shock waves*.

V.I. Rozenband and N. I. Vaganova 1992 *A strength model of heterogeneous ignition of metal particles*, Combust. and Flame 88:113-118.

R.O. Foelsche, R.L. Burton, and H. Krier 1998 *Ignition and combustion of aluminum particles in  $H_2/O_2/N_2$  combustion products*, Journal of Propulsion and Power 117:6:1001-1008.

R.O. Foelsche, R.L. Burton, and H. Krier 1999 *Boron particle ignition and combustion at 30-150 atm*, Combustion and Flame 117:32-58.

S. Gordon and B.J. McBride 1996 *Computer program for calculation of complex chemical equilibrium composition and application*, NASA Reference Publication 1311, Lewis Research Center.

J. Servaites, H. Krier, and J.C. Melcher 2001 *Ignition of aluminum particles in shocked  $H_2O/O_2/Ar$  and  $CO_2/O_2/Ar$  mixtures*, Combustion and Flame 125:1040-1054.